15 INTERNRAPPORT
NORSK POLARINSTITUTT, TROMSØ 2003

Lars Henrik Smedsrud and Hajo Eicken

Report on Sea Ice Data for the KAREX 1994 Expedition

Internrapport nr. 15

Lars Henrik Smedsrud and Hajo Eicken

Report on Sea Ice Data for the KAREX 1994 Expedition

Norsk Polarinstitutt 2003

Addresses:
Lars Henrik Smedsrud
Geophysical Institute
University of Bergen
5000 Bergen
Norway

Hajo Eicken
Alfred-Wegener Institute
Bremerhaven
Germany

Present address:
Geophysical Institute
University of Fairbanks
USA

Norsk Polarinstitutt, Polarmiljøsenteret, NO-9296 Tromsø
www.npolar.no

Cover photo: Hajo Eicken
Technical editor: Gunn Sissel Jaklin
Design: Jan Roald
Printed: Norwegian Polar Institute, October 2003
ISBN: 82-7666-202-1

Contents

Preface

As neither of us took part in KAREX 1994, we were glad to receieve the cores in 1997 and analyse them as discussed with Reinert Korsnes at the Norwegian Polar Institute. The cores showed to be quite interesting and revealed new knowledge about the sediment entrainment processes. The samples are from the north-eastern Kara Sea, and very little is known about sea ice in this region, at least to western scientists.

Much of the ice is granular ice, dynamically grown in open water as frazil ice, with high sediment concentrations. $\delta^{18}O$ values of the sea ice indicate that the ice with the highest sediment concentrations is formed close to the rivers Ob and Yenisey, while the ice with less sediment grows further north.

The ice growth process and entrainment of sediments is discussed using a simple box model, and the onward drift of the ice is followed to the central Barents Sea utilizing satellite derived sea ice motion. This shows that transport of contaminants from the Kara Sea by contaminated sediments is possible, and likely, but to an unknown extent due to the small number of samples.

Lars Henrik Smedsrud and Hajo Eicken

Introduction

The Kara Sea experiences a change from almost 100% ice cover during January through May, to near ice free in late summer. The open northern boundary of the sea is often defined by the 200 m isobath between the northern tip of Novaya Zemlya and Severnaya Zemlya. The ice edge (defined by the 50% concentration line) is found north of the Kara Sea some years in August, while other years it might go as far south as 75º N (Gloersen et al. 1992).

Summer field expeditions are usually too late in the season to sample much ice, leaving our knowledge about the Kara Sea sea ice very limited. The ice core data presented here are few in numbers, but they represent large variations in textural stratigraphy, $\delta^{18}O$ values, and concentrations of Ice Rafted Sediments (IRS).

High variations of $\delta^{18}O$ in sea ice samples from the Kara Sea are expected, due to the large inflow of fresh water from the two rivers Ob and Yenisey, constituting more than 30% of the annual inflow to the Arctic Ocean. The average equivalent thickness of freshwater over the entire Kara Sea is 3.5 m, representing nearly 2.5 years of river discharge (Hanzlick and Aagaard 1980).

High variation in IRS concentration is to be expected all over the Arctic marginal seas due to the entrainment processes, which are probably governed by episodic events. Recent field observations from the central Arctic Ocean and north of Svalbard point to the Kara Sea as a source for IRS with above background concentrations of ^{137} Cs (Cesium) (Meese et al. 1997) and ^{239} Pu (Plutonium) (Landa et al. 1998). This illustrates that contaminants can be transported over very long distances with low diffusion when they are bound to IRS.

How efficient the long range transport of contaminants by the Arctic sea can be in general has been discussed by Pfirman et al. (1995), and for the Kara Sea in particular (Pfirman1997). The potential for transport of contaminants is proportional to the concentrations of IRS, typically ranging between 5 and 500 (Reimnitz et al.1993), (Nurnberg et al. 1994), (Eicken et al. 1995), (Dethleff et al. 1998).

KAREX 1994 was a multi-disciplinary expedition, with the aim to evaluate supplies, distributions, and transport mechanisms for contaminants in the Kara Sea. Observations included suspended particulate matter (SPM), sea bed sediments, fish, and benthic fauna (Evenset et al. 1998), as well as oceanographic observations (Nygaard 1995). Data were collected for hydrocarbons, PCBs, pesticides, metals, organic compounds, and radio nuclides. One of the important qualitative conclusions from the sediment and contaminant analyses was that sediments supplied by river transport to the sea are subsequently incorporated into ice during formation (Evenset et al. 1998). This is supported by the similarity between sediments found in sea ice and the estuaries, and also by the very low sedimentation rates on the Kara Sea shelf in comparison to the large flux of sediments in Ob and Yenisey.

Material and methods

The cores presented here were collected in the north-eastern Kara Sea during August 1994 as a part of KAREX 94. The cruise was a part of the Russian-Norwegian Oceanographic Programme (RUSNOP) and carried out aboard the Russian vessel ''Ivan Petrov''. At three different locations on the shelf, a total of five ice floes was sampled (Figure 1). The dominating floe size at the sites was 20 - 50 m. The sampling was done in the vicinity of the small Sergeya Kirakova islands, at about 100 m depth.

The cores were taken using a standard ice corer with a diameter of 10 cm, put into plastic bags, and stored at -20º C until April 1997. They were then divided vertically in two halves. One half was analysed for sediments and heavy metals at Akvaplan-niva (Evenset et al 1998). The other half was taken to the Alfred Wegener Institute in September 1997 and analysed there for salinity and $\delta^{18}O$.

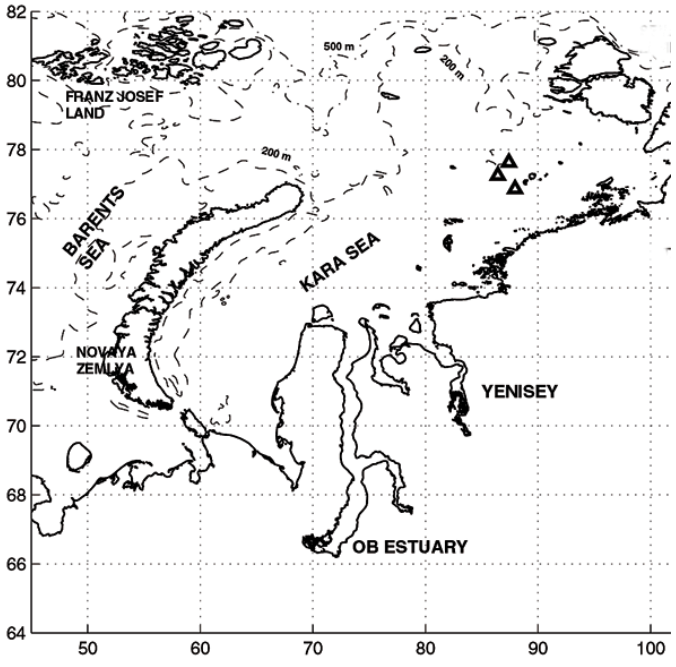

Figure 1
Map of the Kara sea with the ice stations indicated as triangles.

Sediment concentration in the ice was measured by melting the ice, filtering the water on preweighed Nucleopore filters (0.4 μm), and drying the filters at 40º C. When dry, the filters were weighed on a Sartorius micro balance with a static eliminator.
Salinity was measured with a WTW LF2000 conductiv-

ity sensor on melted sections, giving an accuracy of ±0.5 % of the measured value. $\delta^{18}O$ concentrations were determined on ice samples employing an automatic water/carbon dioxide equilibrium system, connected on-line to a Finnigan MAT Delta S mass spectrometer. Measurements were carried out against a laboratory standard, calibrated against IAEA Vienna Standard Mean Ocean Water (VSMOW). For routine measurements the accuracy is < 0.05 promille. The δ-notation indicates the concentration of ^{18}O and ^{16}O in the sample in relation to that of the standard mean ocean water (SMOW) as

$$\delta^{18}O = \left[\frac{\left(\frac{^{18}O}{^{16}O}\right)S}{\left(\frac{^{18}O}{^{16}O}\right)SMOW} \right] 1000\ ‰$$

Results

The small number of samples and the focus on visible sediment laden ice preclude any general conclusions about typical sediment loads or average ice characteristics in the area. Nevertheless, the cores allow conclusions about the origin and sediment entrainment processes.

The samples are examples of sediments in sea ice, and represent high variation in both sediment concentration, textural stratigraphy, $\delta^{18}O$, and metal concentration. This points to the issue of their ''place of growth'' which is discussed later. The focus on sediments and pollutants meant that test cores which showed no sediment inclusion were not continued, and that floes were usually not sampled for their total thickness, leaving this as unknown.

All existing data of sediment concentration, salinity, and $\delta^{18}O$ from the five cores are given in Table 1. General findings are subsequently presented separately for IRS, salinity, and $\delta^{18}O$ data. In addition the two longest cores, Floes 1 and 4, are presented in some more detail.

Table 1
Data sampled from the ice cores

Floe	Depth [cm]	Sediment conc. [mg/l]	Salinity [psu]	$\delta^{18}O$ [‰]
1	13 - 30	5.4	0.2	-0.9009
1	30 - 45	5.4	0.5	0.0401
1	05 - 130	4.6	2.1	0.8968
1	130 - 150	4.6	1.6	1.5388
1	150 - 175	3.8	3.8	0.6451
1	195 - 215	3.8	3.2	-1.0714
1	Mean	4.6	1.9	0.1914
2	1 - 15	2649.6	0.2	-8.6707
2	15 - 23	2583.2	1.1	-11.3354
2	25 - 40	139.9	2.2	-10.3366
2	Mean	1790.9	1.2	-10.1142
4	0 - 20	481.9	0.0	-3.5257
4	20 - 32	229.6	0.1	-4.0469
4	32 - 42	101.1	0.8	-4.0967
4	42 - 58	102.1	1.1	-3.5292
4	58 - 70	132.2	2.4	-3.7866
4	70 - 87	202.1	2.1	-3.4794
4	87 - 95	75.9	4.4	-3.7864
4	95 - 106	75.9	3.1	-4.0812
4	120 - 132	155.0	2.6	-3.897
4	132 - 160	518.4	2.2	-4.4651
4	160 - 187	536.0	3.2	-4.2096
4	187 - 207	305.2	2.8	-3.6565
4	Mean	258.1	1.9	-3.8751
7	0 - 18	5.2	0.1	-4.6681
7	18 - 30	5.2	0.6	-5.0295
7	30 - 42	5.2	2.2	-4.7761
7	120 - 147	24.3	1.8	-2.3867
7	Mean	10.0	1.2	-4.2151
8	0 - 17	4.0	1.5	-4.7444

Positions of floes:
Floes 1 and 2; 76° 52‘ N, 87° 58‘ E,
Floe 4; 77° 38‘ N, 87° 25‘E
Floes 7 and 8; 77° 15‘ N, 86° 26‘ E

Ice rafted sediments

The normal range of IRS in the Arctic (5 - 500 mg/l) (Eicken et al. 95) indicates that the levels presented here are high. The maximum value of 2649.6 mg/l in Floe 2 (Table 1) is one of the highest values of IRS presented from the Siberian shelves (Nürnberg et al. 1994). Levels are often patchy in nature, and the entrainment processes appear to be governed by episodic events according to most researchers. Average values are therefore only locally representative, and to some degree only of temporal validity. A mean value for ''dirty ice'' in the Laptev Sea from August-September 1993 was found to be 156 mg/l (Eicken et al. 1995), and seems to be representative for that area. The overall average of 328.4 mg/l for the five cores presented here should only be used as a value for heavily sediment-laden ice in this particular area. How representative this value is for other seasons, apart from 1993/94, has yet to be confirmed. A study from a lead in

the southern Kara Sea in April, shows values between 2 - 140 mg/l for fast ice and drift ice (about 1 m thick), with an average value of 9.9 mg/l (Dethleff et al. 1998).

For cadmium, copper, lead, and zinc, concentrations were higher on Floes 1 and 7 than on average in the Suspended Particulate Matter (SPM). For the rest of the floes, values were about the same level as in the SPM from the estuaries (Evenset et al 1998).

On Floes 2, 5 and 7 a surface layer of IRS was sampled separately. Floe 5 had the same position as Floe 4 but no core. As this was a larger mass of sediments, additional analysis could be performed on this mass. The surface IRS was fine grained, and more than 90 % of the material was silt or clay (less than 63 μm in diameter). Total organic carbon was close to 2 % dry weight (Evenset et al. 1998). The surface IRS had similar metal concentrations as the core samples. For PCBs and pesticides the values were quite low, although actually among the highest levels found during KAREX 1994. Levels in bottom samples from the shelf and the estuaries were close to the detection limit, while the surface IRS were low in PCB (0,32 to 2,33 μg/kg dry weight), but moderately elevated for HCB (0,14 to 1,27 μg/kg dry weight) and markedly contaminated by DDT (2,75 μg/kg) (Evenset et al. 1998).

The surface IRS might have been transported by winds, but it is most likely that the surface sediment was incorporated into upper parts of the floes, and concentrated near the surface due to surface melt.

Sea ice salinity

August is the end of the melt season in the Kara Sea, and the first day of frost usually falls in September. All of the observed ice is therefore likely to transform to second-year ice, because it has nearly survived one melt season. Second and multi-year sea ice can be distinguished by a rounded, rolling surface of the ice, and a salinity profile increasing from close to zero at the surface to a maximum about 3.5 psu. This salinity profile was found on all the five observed floes. Such a vertical salinity profile is primarily produced by the flushing of nearly pure surface melt water downward through the ice sheet (Weeks and Ackley 1982). The classic C-shape of the vertical salinity profile from new and growing ice was absent in all the cores, and salinity increased almost steadily downwards. The observed profiles were very similar to observations of level summer multi-year ice in the Eurasian sector of the Arctic Ocean (Eicken et al. 1995b).

It is in general difficult to distinguish second and multi-year ice using core data and stratigraphy, especially with such deformed ice as these cores. Salinity profiles generally do not show distinct annual layers. Usually thickness is a good guide for judging the age of sea ice, but we are lacking such data for this expedition.

$\delta^{18}O$ values and parent water masses

Within the Arctic Basin, $\delta^{18}O$ of the sea water increases steadily from the upstream end of the Transpolar Drift. Here, riverine input of meteoric waters highly depleted in $\delta^{18}O$ results in minimum $\delta^{18}O$ sea water composition of around -3 to -5 in the offshore Kara and Laptev Seas.

Ob and Yenisey provide the main supply of freshwater to the Kara Sea with a $\delta^{18}O$ of around -17 (Brezgunov et al. 1983). Water in the Lena river, entering the Arctic Ocean in the Laptev Sea, has a composition between -18 and -21. (Bauch et al. 1995). Towards the Fram Strait the surface water $\delta^{18}O$ increases to above 0 due to the inflow of Atlantic water ($\delta^{18}O$ of roughly 0.3).

The isotopic composition of the cores indicates a growth sequence typical of ice grown in the Arctic Basin or the Kara Sea. Cores from the northern Kara Sea in 1996 showed $\delta^{18}O$ values between 0 and 1.5 (unpublished data). Apart from growth-rate dependent fractionation and other secondary effects, the isotopic composition of Arctic sea ice is determined by the composition of the parent water mass. (This fractionation means that sea water that freezes increases its $\delta^{18}O$ value due to the freezing process.) Fractionation is growth dependent, and ranges mostly between 1.5 and 2.5 promille for $\delta^{18}O$ in thicker Arctic sea ice (Eicken et al. 1997), and (Eicken 1998). To derive the approximate $\delta^{18}O$ value of the parent water mass one therefore needs to subtract a fractionation value of roughly 2, yielding values between a maximum of 0.5 and a minimum of -13.5. Thus Floe 2, with the highest IRS concentration, froze from water composed of more than 50 % river water. Floe 1, with the lowest IRS concentration, formed in sea water with close to Atlantic values of $\delta^{18}O$ (see also Figure 7). This large variation is consistent with observed values of surface salinities in the Kara Sea during summer. The area outside the Ob and Yenisey rivers and estuaries consists of 95 % river water with a salinity of 3-5 psu, and the area north of 77° N consists of less than 5 % river water and has salinities above 30 psu (Pavlov and Pfirman 1995).

Sea ice textural stratigraphy

Although the five ice floes sampled were not more than about 100 km apart, the cores show substantial variations in stratigraphy and ice composition. Except for one core (Floe 6), the majority of the vertical sections show a predominance of granular ice. 71.9 % of the total core length is classified as granular ice, 11.9 % as columnar, and 16.2 % as a mixture of the two, also

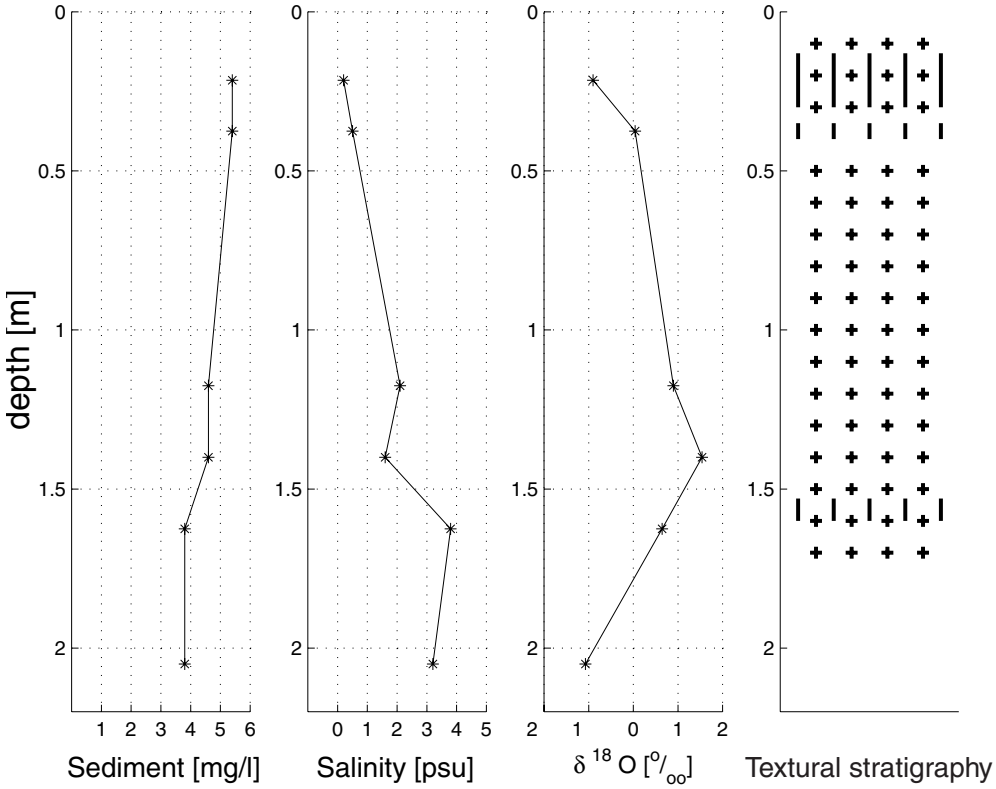

Figure 2
Data from sea ice floe 1. For textural stratigraphy, vertical lines correspond to columnar ice and crosses to granular ice; both crosses and lines represent a mixture of the two ice types.

including pieces of anchor ice in Floe 4. The high portion of granular ice might partially be explained by the selective sampling of ''dirty'' ice floes, as most of the sediment entrainment mechanisms are associated with turbulent conditions, high levels of sediments in suspension, and frazil ice formation, resulting in granular ice texture.

The majority of granular ice types points to such a dynamic ice growth situation for IRS in the Kara sea. This is consistent with similar results from the Laptev Sea, where high IRS concentrations also were associated with dynamically grown ice (Eicken et al. 1997). The observed ice has therefore probably formed during the autumn freeze up, or in leads and polynyas during the previous winter. Much of the ice is deformed and found in shallow layers, with portions of clean ice in between turbid ice with homogeneously distributed sediment inclusions.

Orientation of samples within bags was not indicated during sampling, but this was sometimes possible to identify based on crystal texture. Relative positions of stratigraphic boundaries within individual sample segments may therefore be in reverse depth order.

Detailed description of the core from Floe 1

This core was taken from a 50 m wide floe (76° 52 ‘N, 87° 58 ‘E) appearing almost visually clean. Judging from clear, bubbly ice layers and low salinity in the upper 0.45 m of the core, this may possibly already have been second-year ice, becoming multy-year ice in September 1994. Thus, this ice most likely originated from the northern Kara Sea or the adjacent sector of the Arctic Ocean, also indicated by the high $\delta^{18}O$ values, close to those of Atlantic water. The decrease in $\delta^{18}O$ towards the bottom may reflect decreasing $\delta^{18}O$ of the surface water as the ice was advected from the northern reaches of the Kara Sea and southwards towards the sampling position. The depth variation of the different parameters are shown in Figure 2, and some details are given below:

0.13-0.30 mixed columnar/granular layers of clear ice at 0.13-0.17, 0.19 and 0.22 m (5 mm thick for latter two); in between clusters of bubbles and brine pockets

(0.30 - 0.35) - granular few bubbles and pores

(0.35 - 0.40) - columnar; individual crystals and boundary to granular ice slanted (most likely result of deformation) - clusters of bubbles

(0.40 - 0.45) - granular

(1.05 - 1.30) - granular - small (< 1 mm) bubbles

(1.30 - 1.53) - granular - clusters of pores

(1.53 - 1.60) - mixed columnar/granular; slanted columnar crystals in granular matrix(deformation features)

1.60 - 1.75 - granular - bubbles and arrays of brine pockets and channels.

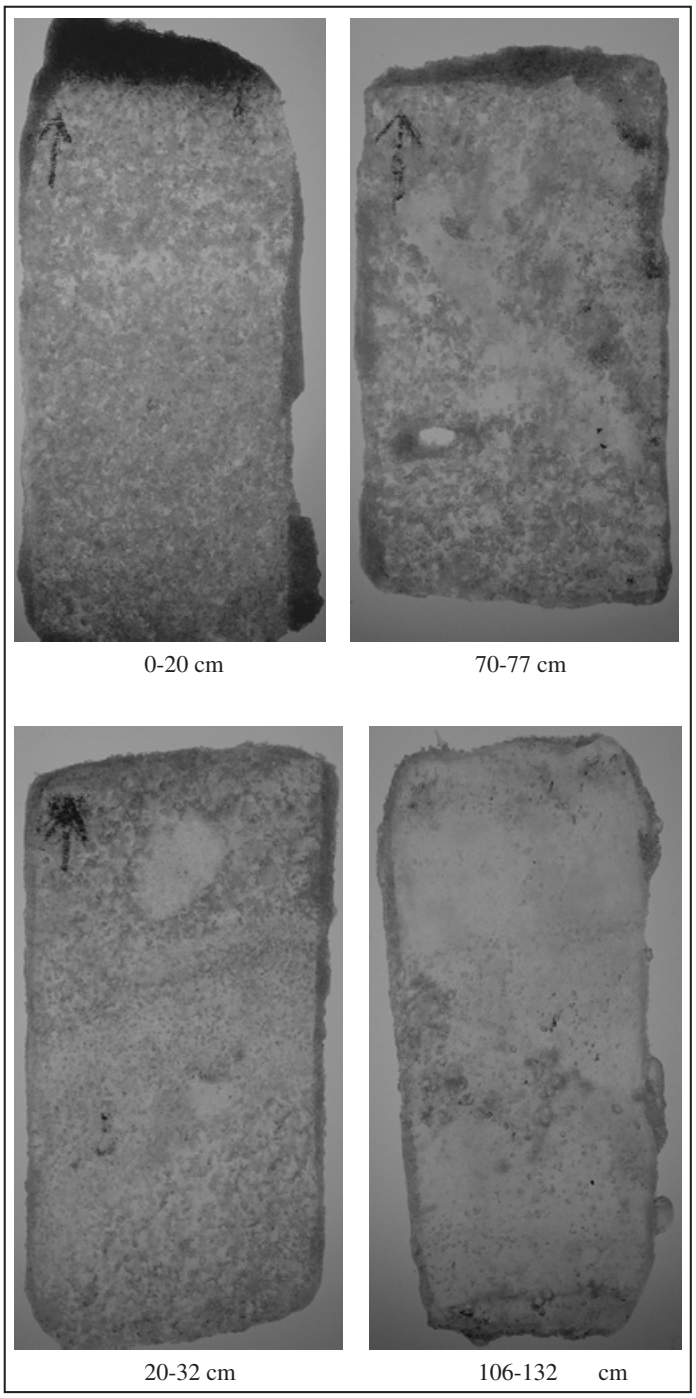

Figure 3
Photos under plain light of thick sections from Floe 4, 0-132 cm. Dark areas are sediment inclusions, the arrow has been drawn with a pencil to indicate upwards direction.

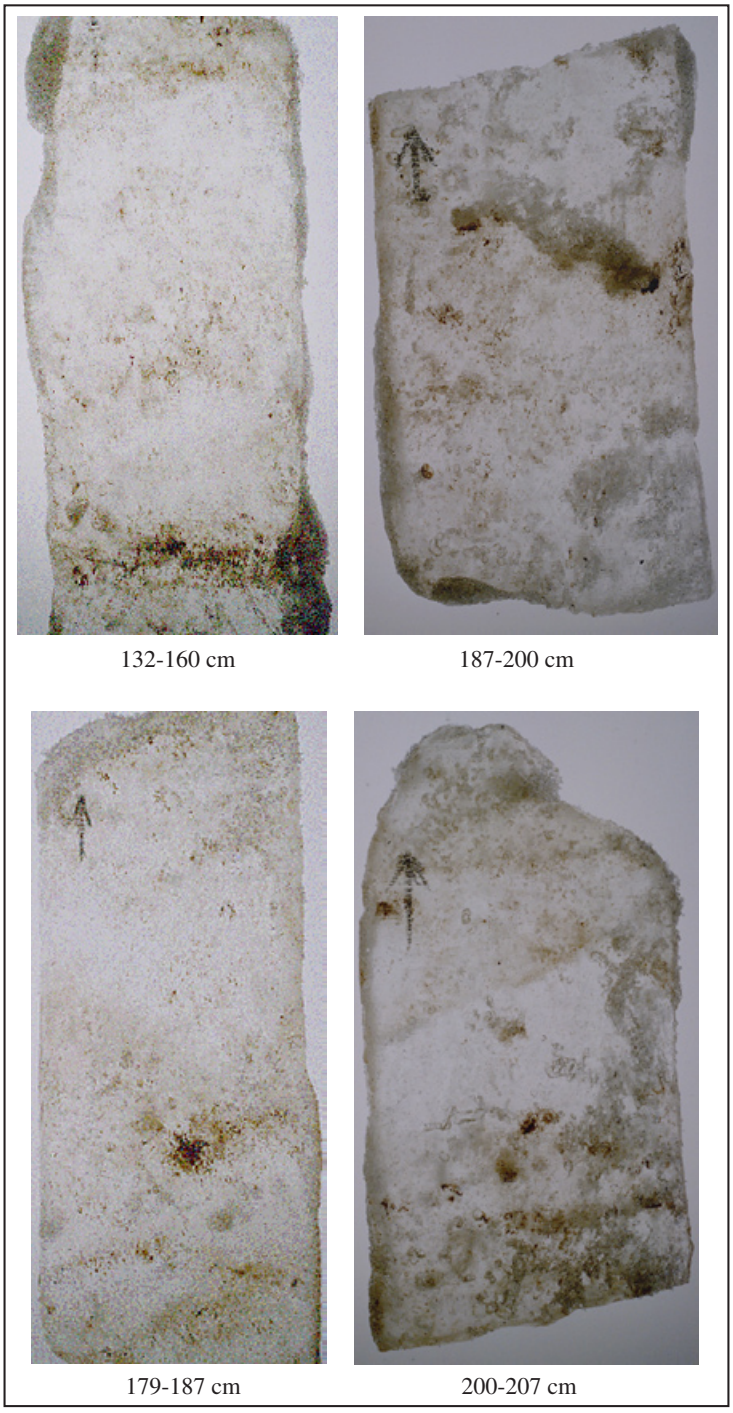

Figure 4
Photos under plain light of thick sections from Floe 4, 132 - 207 cm. Dark areas are sediment inclusions, the arrow has been drawn with a pencil to indicate upwards direction.

Detailed description of the core from Floe 4

This 60 m floe (77° 38 'N, 87° 25 'E) had a cover of IRS on the surface, and a large ridge across it. The ice showed extreme signs of deformation and juxtaposition of different textural units and blocks. The clear ice appeared to be of freshwater origin, and was virtually free of sediment inclusions (Figure 4), (20-32 cm). This freshwater ice was contained within a matrix of ordinary sea ice. Turbid and clean sea ice alternated throughout the core, visible in most segments of the core in Figure 3 and Figure 4. The surface IRS layer was most likely formed as a result of surface melting, which was also indicated by the low surface salinities. Given the high degree of deformation, this ice may have been first-year ice despite its thickness. The appearance of IRS in layers and aggregations in a matrix suggest entrainment of anchor ice into a congealing ice cover. Based on the isotopic composition, ice formation most likely occurred in the far-field influence of a river plume, possibly fairly close to the sampling location. The amount and distribution of sediment suggest formation in shallow water, and under highly turbulent conditions. The depth variation of the different parameters are shown in Figure 5, and a detailed description is found below:

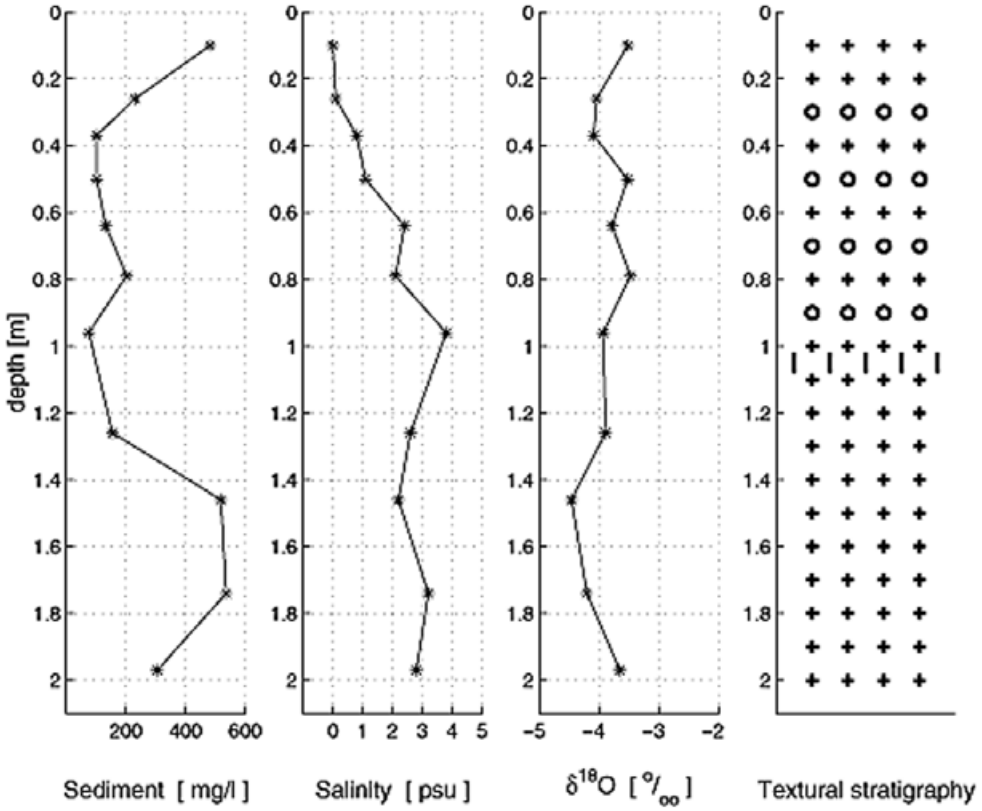

Figure 5
Data from sea ice Floe 4. For textural stratigraphy, vertical lines correspond to columnar ice and crosses to granular ice; both crosses and lines represent a mixture of the two ice types, and rings to anchor/underwater ice.

0.00 - 0.20 - layers and clusters of bubbles - sediment in high concentration at surface (layer 25 mm thick); infiltration of sediment into pores below

0.20 - 0.32 - porous, clear ice with no visible sediment inclusions alternating with clear ice containing few pores and sediment aggregates

0.32 - 0.70 - fine-grained granular - layers of pores - turbid ice with sedimentary particles and aggregates finely dispersed

0.70 - 0.87 - bubbly, clear ice alternating with turbid bubbly ice and clear ice containing sediment aggregates

0.87 - 0.95 - clear ice layer within turbid, bubbly ice; just adjacent (orientation not given on sample bag and difficult to establish) to clear ice sediment accumulated in a layer

0.95 - 1.04 - granular - turbid ice

1.04 - 1.06 - columnar - clear without bubbles or sediment

1.06 - 1.32 - sequence of clear, bubbly ice without sediments and turbid ice; with slanted boundaries separating ice types

1.32 - 1.60 - alternating, slanted layers of granular ice, some coarser grained - turbid ice

1.60 - 1.79 - granular - turbid ice with sediment also occurring in aggregations

1.79 - 1.87 - granular ice - tilted layers of sediments

1.87 - 2.07 - granular - mixed patches of clean and turbid ice

Discussion

To address the questions of origin and onward drift for the sampled floes, the average sea ice drift, as derived from AVHRR images, was utilized (Emery et al. 1997). The sediment entrainment processes are discussed, and finally simple estimates of the SPM levels during the entrainment episodes are given.

Satellite derived ice drift analyses

The seven year average (1988 - 1994) in the AVHRR Polar Path finder data shows a distinct mean flow of sea ice from the Kara Sea, northwards to about 80° N, then westwards around Novaya Zemlya, and later southwest into the Barents Sea south of Franz Josef Land. In 1994 this part of the mean drift was particularly strong, as can be seen in Figure 6 mean. The ice originating east of about 80° E tended to drift directly north, entering the Arctic Ocean between Franz Josef Land and Severnaya Zemlya, and then turning south east. This ice either entered the Barents Sea between Franz Josef Land and Svalbard, or the Greenland Sea in Fram Strait. Sea ice originating just north of the Ob estuary will on average travel to a central location in the Barents Sea (76° N, 40° E) in about two years. The variance shows that for a two year drift, the ice could end up anywhere between Severnaya Zemlya and Bjørnøya south in the Barents Sea, well across the polar front, where ice melts rapidly.

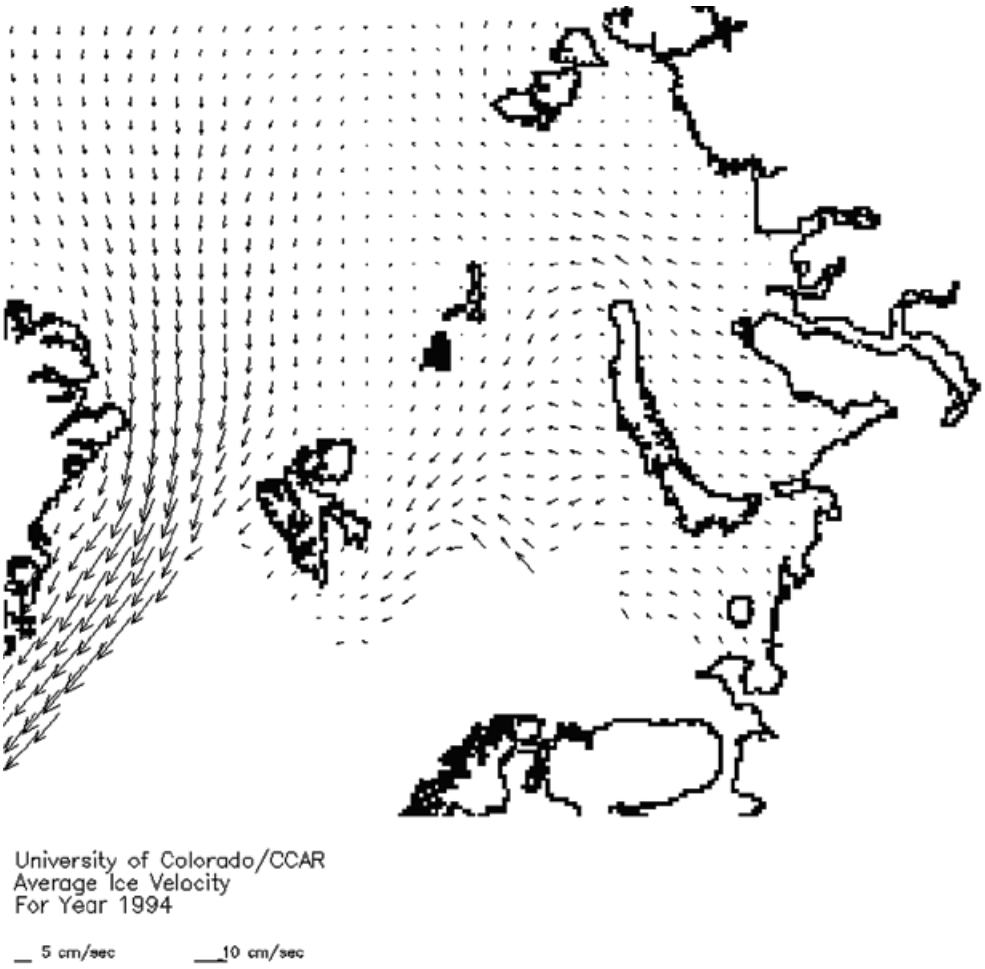

Figure 6
Average ice velocity for 1994. University of Colorado/CCAR, AVHRR

The AVHRR Polar Pathfinder backward drift simulation indicates that the floes sampled during KAREX 1994 originated closer to the coast than where they were sampled. Positions indicated for October 1993 are from north of the Yenisey (75° N, 78° E) to Vilkitsky Strait between Severnaya Zemlya and the coast (77° N, 94° E). Following the sampled floes into the next winter, they drift almost directly northward, ending at about 80° N by summer 1995. The ice was thus probably integrated into the Transpolar drift, and ended up in the Barents Sea, after one or two more years. It has to be emphasized that this forward simulation is using the average monthly mean drift for several years, and the variance over such a long time is large. The indicated possible final positions for the cores are from the Fram Strait to Franz Josef Land, Novaya Zemlya, or Severnaya Zemlya. In fact the ice could also end up near the coast in the Kara Sea, close to where it most probably grew.

The results from the AVHRR Polar Pathfinder is consistent with those found using data from the International Arctic Buoy Program (Pfirman 1997b). In this study sediment composition and Planktonic freshwater diatoms were also utilized as tracers, concluding that the Kara Sea is a major contributor of ice to the Barents Sea and the southern limb of the Transpolar Drift Stream.

Sediment entrainment mechanisms

From the limited number of samples available in this study, it is clear that nearly all the IRS is found within granular ice. This is consistent with similar results from the Laptev and Beaufort Seas (Eicken 1997), (Osterkamp 1984). In addition, anchor ice was tentatively identified in Floe 4. This is consistent with direct observations of anchor ice with incorporated sediments from sites shallower than 20 m in the Beaufort Sea (Reimnitz 1987). Thus it appears as if the same processes are taking place in the Kara Sea.

Indirect measurements such as these seem to support the ''scavenging process'' theory (Osterkamp 1984). During this process frazil crystals form in open water slightly below the freezing point (super cooled) due to a strong heat flux to the cold air above. If the wind and currents are strong enough, the crystals will diffuse downward and scavenge the water column, collecting sediment grains on their way through the water. High concentrations of sediment (SPM) are only expected in shallow water (50 m). If any of the crystals diffuse down to the bottom, anchor ice may form (ice attached to the bed). Anchor ice may then grow in volume by both additional attachment of new crystals, or by direct freezing if the water is super cooled at that depth. The process is sometimes referred to as ''Suspension

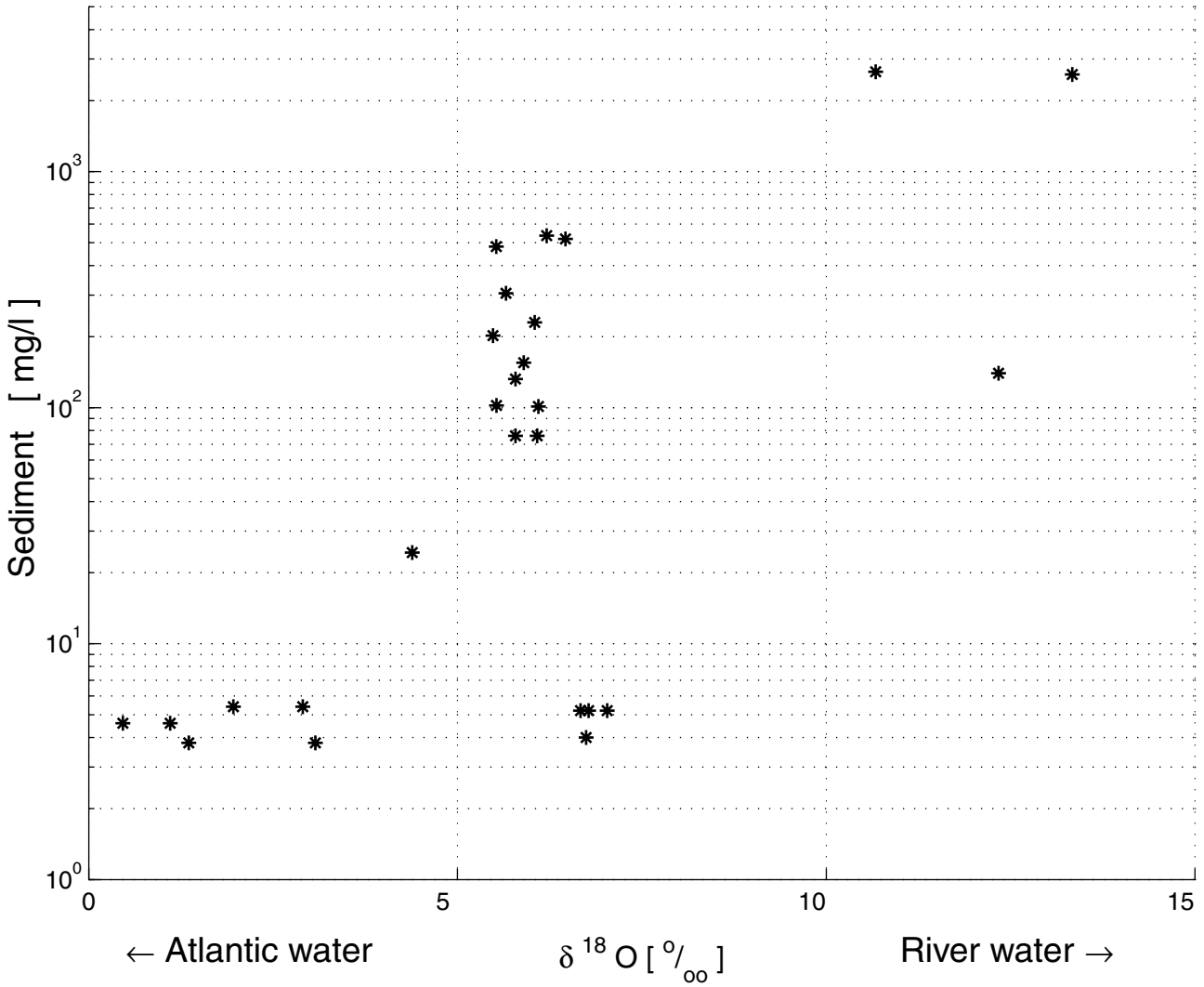

Figure 7
Plot of all available $\delta^{18}O$ values versus sediment concentrations from Table 1. The $\delta^{18}O$ values have been subtracted a mean fractionation value of 2 to make them directly comparable to water values.

freezing'', including scavenging and anchor ice formation. Laboratory work has shown that scavenging takes place under special conditions (Reimnitz 1993), and the efficiency of the scavenging process was estimated by use a box-model and laboratory results (Smedsrud 1998).

Given a situation where frazil forms, the IRS concentration in the growing ice cover will to a first approximation be controlled by the SPM concentration in the water. This is usually not known, and in general it might change during the ice formation as well. As with the cores presented here, no precise information about the location and conditions the ice formed under during winter 1993 is known, except for the $\delta^{18}O$ values.

Figure 7 shows that the IRS concentration increases with decreasing $\delta^{18}O$ values. IRS concentrations lower than 10 mg/l are associated with water close to Atlantic origin, while higher IRS concentrations are associated with lower $\delta^{18}O$ values and thereby water containing between 30 and 50 % river water ($\delta^{18}O$ around -17). There is only an indirect link between the two parameters; River water flows generally to the right from the river deltas of Ob and Yenisey, and along the coast in fairly shallow water (<50 m) mixing gradually with the Atlantic water (Pavlov 1995). During summer the area with >25 river water extends almost all the way to the sea ice sampling location (Figure 1). Sea ice that grows in this water is therefore formed in shallow water, and is likely to have high SPM concentrations during strong wind events, when sediments re-suspend from the combined effect of currents and waves (Sherwood 2000). The area between the rivers and the sampling location is also the area with a reoccuring polynya during winter (Pavlov 1995).

From Figure 7 it is obvious that not all of the low $\delta^{18}O$ values are associated with high IRS concentrations. This is probably ice that formed from water with lower SPM concentrations, and during relatively calm conditions. Figure 7 also shows that there are no samples of ice

formed from Atlantic water with high IRS concentration. This indicates that even with dynamic ice formation, the granular ice ends up with low IRS levels when formed in deep water with associated low levels of SPM.

Box-model entrainment calculations

To address the questions of the entrainment process further, and to compare the field data with laboratory experiments, a simple box-model was utilized (Smedsrud 1998). The model treats the water column as homogeneous, and calculates the volume of sediments aggregated to suspended frazil, based on sediment concentration in the water, turbulence intensity (turbulent dissipation rate), and the ice production. An estimate of the mean sediment and frazil size is also needed.

The term ''aggregation'' is preferred when describing the bonding between sediment and crystals. Aggregation is a general term, covering both flocculation (physical bonding), and coagulation (a weaker bonding with a liquid film between). In addition, aggregation is here taken to also include mechanical trapping of sediments by the frazil crystal. The mean entrained IRS found in Floe 1 was 4.6 mg/l, and in Floe 4 it was 258.1 mg/l. How does this fit with ''normal'' atmospheric forcing over Arctic leads, and the range in observed SPM concentrations?

Both of these cores consisted of deformed ice, and it is likely that the original thickness of frazil or slush was less than the length of the core at the end of the entrainment episode. From the core stratigraphy, at least three different layers were evident, so a thickness of 50 cm of original frazil slush were used as a final state for the box model. In this surface slush, a frazil ice concentration of 120 g/l was assumed, similar to what was found during the Interice I laboratory experiments.

For these calculations, the heat flux was set to 200 W/ m^2. This is a normal value, comparable to an air temperature of ~10° C and a wind speed of 20 m/s using standard bulk formulas (Gill 1982). The mixed layer with homogeneous concentrations of frazil and sediment was set to 20 m depth, comparable to the water depth close to the Kara Sea rivers, and to the upper mixed layer of the Kara Sea (Nygaard 1995).

Following Smedsrud (1998), the heat flux produces frazil ice modelled as spheres with a radius of 500 µm with a constant rate. This ice production amounts to 4.22 x 10^{-8} $[(m^3/m^3)s^{-1}]$ or 2.8 kg/ (m^2 hour) from the 200 W/m^2. All of this ice is modelled as in homogeneous suspension due to the wind speed of 20 m/s, creating waves, breaking waves and shear. After 24 hours, the suspended frazil ice concentration over the 20 m will be 3 g/l. The wind is then ''switched off'', and the frazil crystals permitted to rise with their aggregated sediments, forming the 50 cm slush layer.

The wind creates turbulence modelled by the turbulent dissipation rate, and estimated as 10° C, -5 W/kg. Sediments are modelled as spheres with a mean radii of ~ 2.5µm. Sensitivity analyses using a mean radius for sediments and frazil ice show that the modelled aggregation is not particularly sensitive to the choice of the mean radius (Smedsrud 1998). The most sensitive parameter in estimating the aggregation factor proved to be the turbulence. In our calculations here, an aggregation factor α 0.003 is used. The box model was used to estimate the sediment concentration in the water during the scavenging process, and this turned out to be quite different between the two cases.

For Floe 1, which formed in water close to Atlantic origin, probably in deep water, far from the river estuaries, an initial sediment concentration in the water of about 5 mg/l was found. For Floe 4, which formed in about 30 % river water, probably in shallow water (< 50 m) on the Kara Sea shelf, this was increased to 200 mg/l. The calculated SPM concentration of 200 mg/l is a high value, but still within observed values from the Beaufort Sea at shallow depths (<5 m) during strong wind episodes (Kempema et al. 1989). Alternatively a more shallow depth could be chosen for the Floe 4 case, making it more likely that such high sediment concentrations would occur. In addition, the simple box model does not account for the observed anchor ice that formed at Floe 4. Anchor ice would definitely increase the efficiency of the sediment entrainment process, and this is a process which should be incorporated into more advanced future models of the entrainment processes.

Nevertheless, these simple calculations show that the scavenging process is capable of producing observed loads of IRS.

Concluding remarks

For some years, it has been assumed, or speculated, that sea ice can transport a lot of sediments and bonded contaminants from the Kara Sea to the Barents Sea or the Arctic Ocean. The cores presented here confirm that very high levels of IRS can be found in the Kara Sea. The $\delta^{18}O$ values indicate that the sampled sea ice with highest IRS concentration was formed in water consisiting of more than 50 % river water. Such water masses are generally found close to the coast on shallow depths.

For the sea ice with low levels of IRS, $\delta^{18}O$ values indicate growth in Atlantic water, with minor influence of other water masses. Such water masses are mainly found north in the Kara Sea, and off the continental shelf.

The ice drift analyses confirmed that this sampled ice was likely to drift into the Barents Sea, and melt somewhere in the Polar front were much of the sediments and the bonded contaminants would be released.

The entrainment calculations indicate that the modelled process is capable of producing the observed concentration of IRS, but also other processes are probably important, for instance anchor ice formation that was identified in these samples.

How representative these values and calculations are, is a very important and difficult question to answer, and can only be addressed with more sampling of sea ice in the Kara and Barents Seas, and more realistic modelling using observed data of the sea ice cover, local atmospheric forcing, and oceanographic data during the entrainment events in the winter season.

Acknowledgements

The authors would like to thank Reinert Korsnes at the Norwegian Polar Institute for making the cores available to us, and Anita Evenset at Akvaplan-niva for providing thesediment data. We are also grateful for the good technical assistance we received at the Alfred Wegener Institute ice laboratory. The AVHRR Polar Path Finder figure and results were found at the University of Colorado http://polarbear.colorado.edu/, AVHRR Polar Pathfinder. This work was supported by the Norwegian Research Council, under contract No 71928/410.

References

Bauch, D., P. Schlosser, and R. G. Fairbanks, (1995). Freshwater balance and the sources of deep and bottom waters in the Arctic Ocean inferred from the distribution of H218O. Prog. Oceanog. 35, 53 - 80.

Brezgunov, V., V. Debol'skii, V. V. Nechaev, V. I. Ferronski, and T. V. Yakimova (1983). Characteristics of the formation of the oxygen isotope composition and salinity upon mixing of sea and river waters in the Barents and Kara Seas. Water Resources, (translation of Vodn. Resurs.) 9, 335 - 344.

Dethleff, D., P. Löwe, H. Weilel, D. Nies, G. Kuhlmann, C. Bahe, and G. Tarasov (1998). KaBaEx '97 Winter Expedition to the Southwestern Kara Sea - Investigations on Formation and Transport of Turbid Sea-Ice. Unpublished.

Eicken, H. (1998). Factors determining microstructure, salinity and stable-isotope composition of Antarctic sea ice: Deriving models and rates of ice growth in the Weddell Sea. AGU Antarct. Res. Ser.

Eicken, H., M. Lensu, W. Tucker, A. Gow, and O. Salmela (1995 b). Thickness, structure, and properties of level summer multiyear ice in the Eurasian sector of the Arctic Ocean. Journal of Geophysical Research, 100, C 11, 22697 - 22710.

Eicken, H., E. Reimnitz, V. Alexandrov, H. Martin, T. Kassens, and T. Viehoff (1997). Sea-ice processes in the Laptev Sea and their importance for sediment export. Continental Shelf Research, 17, 205-233.

Eicken, H., T. Viehoff, T. Martin, J. Kolatschek, V. Alexandrov, and E. Reimnitz (1995). Studies of clean and sediment-laden ice in the Laptev Sea. In H. Kassens, D. Piepenburg, J. Thiede, L. Timokhov, H. Hubberten, and S. M. Priamikov (Eds.), Reports on Polar Research no.176 - Laptev Sea System, pp. 62-70. Bremerhaven, Federal Republic of Germany: Alfred Wegener Institute for Polar and Marine Research.

Eicken, H., J. Weissenberger, J. Freitag, W. Schuster, F. Valero-Delgrado, K. U. Evers, P. Jochmann, C. Krembs, R. Gradinger, F. Lindemann, F. Cottier, R. Hall, P. Wadhams, M. Reisemann, H. Kousa, J. Ikavalko, G. H. Leonard, H. Shen, S. F. Ackley, and L. H. Smedsrud (1998). Ice-tank studies of physical and biological sea-ice processes}. In H. Shen (Ed.), Ice in Surface Waters, pp. 363-370. A.A. Balkema, Rotterdam. International Association for Hydraulic Research - 14th International Symposium on Ice.

Emery, W. J., C. W. Fowler, and J. A. Maslanik (1997). Satellite-derived maps of Arctic and Antarctic sea ice motion: 1988 to 1994. Geophysical Research Letters, 24, 897 - 900.

Evenset, A., S. Dahle, D. Loring, J. Skei, K. Sørensen, S. Cochrane, J. Carroll, and C. Forsberg (1998). KAREX 94: An environmental survey of the Kara Sea and the estuaries of Ob and Yensiey, Akvaplan-niva.

Gill, A. E. (1982). Atmosphere-Ocean Dynamics, Volume 30 of International Geophysics Series, Academic Press, Inc.

Gloersen, P., W. J. Campbell, D. J. Cavalieri, J. C. Comiso, C. L. Parkison, and H. J. Zwally (1992). Arctic and Antarctic sea ice, 1978 - 1987. National Aeronautics and Space Administration, Washington, D.C.

Hanzlick, D. and K. Aagaard (1980). Freshwater and Atlantic water in the Kara sea. Journal of Geophysical Research 85, C 9, 4937-4942.

Kempema, E. W., E. Reimnitz, and P. W. Barnes (1989). Sea Ice Sediment Entrainment and Rafting in the Arctic. Journal of Sediment Petrology, 59, 308-317.

Landa, E. R., E. Reimnitz, D. M. Beals, J. M. Pochkowski, W. G. Winn, and I. Rigor (1998). Transport of 137 CS and 239, 240 Pu with Ice-rafted Debris in the Arctic Ocean. Arctic, 51, 27-39.

Meese, D. A., E. Reimnitz, W. B. Tucker, A. J. Gow, J. Bischof, and D. Darby (1997). Evidence for radionuclide transport by sea ice. Science of the Total Environment, 202, 267-278.

Nürnberg, D., I. Wollenburg, D. Dethleff, H. Eicken, H. Kassens, T. Letzig, E. Reimnitz, and J. Thiede (1994). Sediments in Arctic sea ice: Implications for entrainment, transport and release. Marine Geology, 119, 184-214.

Nygaard, E. (1995). Ctd-report from KAREX 94. Rapportserie, nr. 90, Norsk Polarinstitutt.

Oakey, N. S. and J. A. Elliott (1982). Dissipation Within the Surface Mixed Layer. Journal of Physical Oceanography, 12, 171-185.

Osterkamp, T. E. and J. P. Gosink (1984). Observations and analyses of sediment-laden sea ice. In P. Barnes, D. Schnell, and E. Reimnitz (Eds.), The Alaskan Beufort Sea: Ecosystems and Environments, pp. 73 - 93. Academic Press, Orlando.

Pavlov, V. K. and S. L. Pfirman (1995). Hydrographic structure and Variability of the Kara Sea: Implication for pollutant distribution. Deep Sea Research II, 42, (6), 1369 -1390.

Pfirman, S., H. Eicken, D. Bauch, and W. F. Weeks (1995). The potential transport of pollutants by Arctic sea ice. Science of the Total Environment, 159, 129 - 146.

Pfirman, S., J. W. Kogeler, and I. Rigor (1997). Potential for rapid transport of contaminants from the Kara Sea. Science of the Total Environment, 202, 111 - 122.

Pfirman, S., R. Colony, D. Nürnberg, H. Eicken, and I. Rigor (1997 b). Reconstructing the origin and trajectory of drifting Arctic sea ice. Journal of Geophysical Research, 102, C 6, 12575-12586.

Reimnitz, E., J. R. Clayton, E. W. Kempema, J. R. Payne, and W. S. Weber (1993). Interacting of rising frazil with suspended particles: tank experiments with applications to nature. Cold Regions Science and Technology, 21, 117-135.

Reimnitz, E., E. W. Kempema, and P. W. Barnes (1987). Anchor Ice, Seabed Freezing, and Sediment Dynamics in Shallow Arctic Seas. Journal of Geophysical Research, 92, C 13, 14671-14678.

Reimnitz, E., M. McCormick, K. McDougall, and E. Brouwers (1993). Sediment Export by Ice Rafting from a Coastal Polynya, Arctic Alaska, U.S.A. Arctic and Alpine Research, 25, 83-98.

Sherwood, C. R. (2000). Numerical Model of Frazil-Ice and Suspended-Sediment Concentrations, and Formation of Sediment-Laden Ice in the Kara Sea. Journal of Geophysical Research. 105 (C6) 14061 - 14080.

Smedsrud, L. H. (1998). Estimating aggregation between suspended sediments and frazil ice. Geophysical Research Letters, 25, (20) 3875 -3878.

Weeks, W. F. and S. F. Ackley (1982). The growth, structure, and properties of sea ice. CRREL monograph 82 - 1, Cold Regions Research & Engineering Laboratory, Hanover, New Hampshire, U.S.A.